Synthesis, Characterization and Electronic Properties of some Hetero-arylene Vinylene Oligomers

Johan F.A. Van Der Looy, Gerd J.H. Thys, Pieter E.M. Dieltiens, Daniël De Schrijver, Christian Van Alsenoy, Herman J. Geise*

University of Antwerpen (UIA), Department of Chemistry, Universiteitsplein 1; B-2610 Antwerpen (Wilrijk); Belgium

Abstract: The synthesis and characterization is reported of six 2,5-distyryl-heteroarylenes (BXB compounds) and 1,4-bis{2-(heteroaryl-2-yl) ethenyl}benzenes (XBX compounds) containing the thienyl, furanyl or *N*-methylpyrryl as the heteroarylene moiety. By means of NMR and UV/Vis spectroscopy the electronic structure was probed. Quantum mechanical calculations using the semiempirical CNDO/S-CI approach rationalize the experimental findings and support the peak assignments. © 1997 Elsevier Science Ltd.

INTRODUCTION

Interest in π-conjugated oligomers has steeply increased over the past decade, not in the least because of their potential applications in opto-electronic industry. Among such oligomers, hetero-arylene vinylene trimers - i.e. compounds containing three arylene rings connected through vinylene (-CH=CH-) links - are not yet extensively investigated, despite expectations of interesting electronic properties resulting from a dense and highly polarisable π-electron system. Therefore, we report the results of an investigation of two series of mixed trimers: 1,4-bis{2-(heteroaryl-2-yl)ethenyl}benzenes (XBX series) and 2,5-distyrylheteroarylenes (BXB series). Figure 1 gives structural formulas and abbreviations as well as their synthesis via the Wittig reaction. The compounds were characterized from mass spectrometry and NMR spectra. The latter in combination with UV/Vis spectroscopy was used to probe the electronic structure. To rationalize the observations quantum mechanical calculations were performed. The geometries of the molecules were optimized using the semiempirical AM1 approach[1]. The optimized geometries were used in single-point CNDO/S-CI calculations to rationalize the λ_{max} phenomena and to support the peak assignments.

SYNTHESIS

All trimers were prepared via the Wittig reaction as outlined in Figure 1. The reaction results in a mixture of cis,cis-, cis,trans-, and trans,trans-isomers which were isomerized into the pure trans,trans-isomers by refluxing the mixture in toluene in the presence of a catalytic amount of iodine. It may be noted that two Wittig pathways may lead to the same symmetric trimer: one may select (i) a dialdehyde to react with a
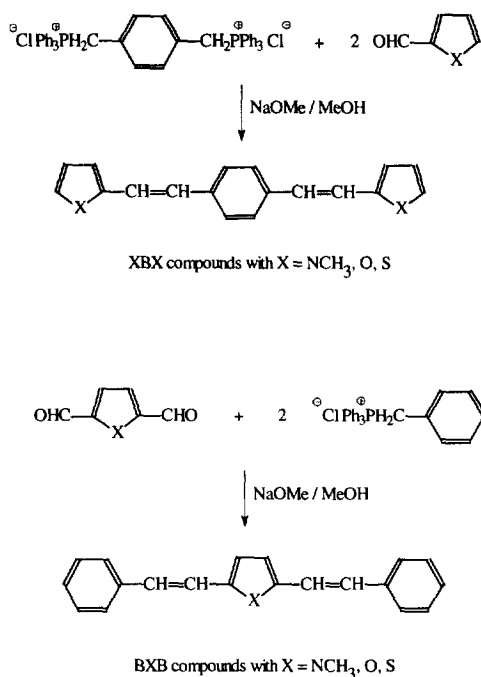
Figure 1: *Structural Formulas and Abbreviations of the Compounds Together with their Synthesis via the Wittig Reaction Route.*

monophosphonium salt or (ii) a bisphosphonium salt to react with a monoaldehyde. If a heterocyclic ring forms the central part - as in compounds BXB - the better strategy is to react a 2,5-heterocyclic dialdehyde with phenylmethylene(triphenyl-phosphonium chloride). The reason is that 2,5-heterocyclic bisphosphonium salts eliminate triphenylphosphine more easily than their phenyl analogues[2-5]. The elimination leads to a 2-methyl-5-methylene (triphenylphosphonium chloride) substituted heterocycle, which in turn may produce a dimer. The activated 2-CH_3 group may even cause polymerisation of the 2-methyl-5-phosphonium salt[2]. To avoid such problems route (i) was chosen. The required 2,5-dialdehydes were prepared from thiophene and N-methylpyrrole following a route published by Feringa et al[6] with yields of 65 % and 40 %, respectively. An excellent route to furan-2,5-dialdehyde is the oxidation of 2,5-furandimethanol using activated MnO_2 in benzene. The yield is almost quantitative[7-8].

Synthesis Experimental

   N-methylpyrrole-2,5-dialdehyde. Under nitrogen protection, 0.11 mol n-butyllithium (44 ml of a 2.5M n-BuLi solution in hexane) is diluted with 85 ml hexane and this solution is added dropwise to a solution of 0.05 mol (4.1 g) N-methylpyrrole and 0.11 mol (13.8 g) tetramethyl ethylene diamine in 15 ml hexane. After refluxing for 3 hours, the reaction mixture is cooled to room temperature and 60 ml of tetrahydrofuran is added in one portion. Then, 0.1 mol (7.3 g) dimethylformamide is added dropwise after the mixture is cooled to -10°C. The ice bath is removed and the mixture refluxed for 30 min. Finally, the reaction is quenched by pouring the reaction mixture into a solution of 90 ml 30 % hydrochloric acid in 850 ml water at -5°C. With a saturated

NaOH solution the reaction mixture is brought to pH = 6. The precipitate is filtered off, and the filtrate extracted with ether. The combined organic layers are dried over anhydrous $MgSO_4$ and the solvent is evaporated. The crude product is purified by crystallisation from hexane, to give a yield of 40 % (2.8 g), with mp. 94-95°C.

1,4-bis{2-(N-methylpyrrole-2-yl)ethenyl}benzene, NBN. In 100 ml ethanol are solved 0.023 mol (16.1 g) p-xylyltriphenylphosphonium chloride and 0.046 mol (5.0 g) N-methylpyrrole-2-aldehyde. Under nitrogen protection, 50 ml of a 1 M sodium methoxide solution in methanol is added dropwise. The precipitate is collected and washed with warm water, while an additional amount of NBN is obtained by adding water to the filtrate. The crude product is purified by Soxhlet extraction using a water : methanol (1:1) mixture. The pure NBN decomposes without melting at 280°C; yield : 50 % (6.6 g). Compound OBO was prepared according to De Schrijver [9], compound SBS according to Sprangler et al [10], and compounds BNB, BOB and BSB according to Seus [11]. Table 1 gives the melting points.

Table 1: *Melting Points of Compounds.*

Compound	mp (°C)	Compound	mp (°C)
NBN	>280 (decomp.)	BNB	190-191 (192[c])
OBO	208-209 (208[a])	BOB	143-144 (144-145.5[c])
SBS	263-264 (264-265 [b])	BSB	189-191

[a] taken from ref. [9], [b] taken from ref. [10], [c] taken from ref. [11]

Mass spectrometry

Electron impact spectra (70 eV) were recorded on a VEQ-70 hybrid spectrometer. The m/z-values and relative abundances of the major peaks are summarized in Table 2. In all cases the molecular ion was found to be the base peak, and the M^{2+} ion was also clearly visible with abundances between 5 and 18 %. This already shows the stability of the M^+ ion and consequently fragment ions have low intensities. Nevertheless, one may note some interesting similarities and dissimilarities between the molecules. For example, all compounds fragment to give ions at m/z = 165 ($C_{13}H_9$) and m/z = 152 ($C_{12}H_8$), possibly benzindene and acenaphtene type ions, formed by cyclization and aromatization arising out of one styryl moiety and 4 or 3 carbon atoms of the neighbouring heterocyclic ring. In case a hetero-atom participates in such a cyclization, one expects and indeed observes ions such as $C_{13}H_9NH$ (m/z = 180), $C_{13}H_9O$ (m/z = 181), $C_{13}H_9S$ (m/z = 197) and $C_{12}H_8NH$ (m/z = 167). Furthermore, all molecular ions lose a H radical, the expulsion being more important in BXB compounds than in XBX compounds.

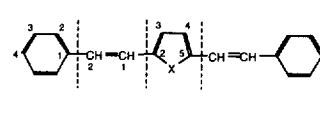Other more convincing distinctions between a molecule of the XBX series and its counterpart in the BXB series are: (i) the loss of C_7H_7 (M-91) from BXB, compared to the loss of C_6H_6N (M-92) from NBN, and of C_6H_6S (M-110) from SBS. Compound OBO does not expel a similar seven membered ring. (ii) the appearance of a signal at m/z = 91 (C_7H_7) from BXB compounds compared to the appearance of one at m/z = 94 ($C_6H_6NH_2$) in NBN, and one at m/z = 109 (C_6H_5S) in SBS. The latter results from fission of the bond between the olefinic link and the central phenyl ring. It also seems that peripheral heterocyclic rings fragment more easily than central ones. For example, in the spectrum of NBN we observe ions at m/z = 231 (M - $CH_2=NHCH_3$ - CH) and at m/z = 218 (M - $CH_2=NHCH_3$ - C_2H_2), which do not occur in BNB. Similarly, expulsions in OBO lead to ions at m/z = 233 (M - CHO), m/z = 205 (M - CHO - CO) and m/z = 179 (M - HCO - CO - C_2H_2), none of which is seen in BOB. Furthermore, such a characteristic expulsion in SBS results in an ion at m/z = 234 (M - H_2S - C_2H_2) which

does not occur in BSB. Typical for the thiophene containing trimers is the loss of H_2S. The most striking phenomenon in the spectra of the furan trimers is the lack of oxygen-containing fragments below m/z = 200, thus showing the ease with which the furan ring fragments under electron impact.

Table 2: *Electron Impact (70 eV) Mass Spectra. m/z Values with Relative Abundances (%) in Parentheses.*

NBN		OBO		SBS	
288 (100)	M^{+}	262 (100)	M^{+}	294 (100)	M^{+}
144 (9)	M^{2+}	131 (9)	M^{2+}	147 (18)	M^{2+} and/or C_9H_7S
287 (9)	M-H	261 (1)	M-H	293 (9)	M-H
231 (5)	$M-H_2CNCH_3-CH$	233 (8)	$M-CHO \equiv F$	260 (14)	$M-H_2S$
218 (5)	$M-H_2CNCH_3-C_2H_2$	205 (11)	F-CO	259 (15)	$M-H_2S-H$
206 (13)	M-A-2H	179 (9)	$F-CO-C_2H_2$	258 (130)	$M-H_2S-2H$
196 (11)	$M-C_6H_6N$	178 (10)	$F-HCO-C_2H_2$ ($C_{14}H_{10}$)	234 (9)	$M-H_2S-C_2H_2$
180 (5)	$C_{13}H_9NH$	165 (9)	$C_{13}H_9$	227 (10)	$C_{18}H_{11}$
167 (6)	$C_{12}H_8NH$	152 (7)	$C_{12}H_8$	209 (12)	$C_{14}H_9S$
165 (6)	$C_{13}H_9$			208 (11)	$C_{14}H_8S$
152 (5)	$C_{12}H_8$			197 (11)	$C_{13}H_9S$
115 (8)	C_9H_7			184 (18)	$C_{12}H_8S$
94 (5)	$C_6H_6NH_2$			165 (7)	$C_{13}H_9$
A : $C_4H_4NCH_3$				152 (8)	$C_{12}H_8$
BNB		BOB		BSB	
285 (100)	M^{+}	272 (100)	M^{+}	288 (100)	M^{+}
142.5 (7)	M^{2+}	136 (7)	M^{2+}	144 (5)	M^{2+}
284 (22)	M-H	271 (7)	M-H	287 (7)	M-H
208 (10)	$M-C_6H_5$	181 (11)	$M-C_7H_7$ $C_{13}H_9O$	254 (16)	$M-H_2S$
194 (20)	$M-C_7H_7$	165 (8)	$C_{13}H_9$	253 (17)	$M-H_2S-H$
180 (8)	$C_{13}H_9NH$	152 (3)	$C_{12}H_8$	252 (15)	$M-H_2S-2H$
167 (7)	$C_{12}H_{10}NH$	115 (12)	C_9H_7	239 (10)	$C_{19}H_{11}$
165 (7)	$C_{13}H_9$	103 (11)	$C_8H_7 \equiv A$	197 (5)	$M-C_7H_7$
152 (4)	$C_{12}H_8$	91 (11)	C_7H_7	184 (7)	$C_{12}H_8S$
115 (12)	C_9H_7	77 (10)	C_6H_5	165 (7)	$C_{13}H_9$
91 (12)	C_7H_7			152 (6)	$C_{12}H_8$
				147 (9)	C_9H_7S
		A : $C_6H_5-CH=CH-$		115 (10)	C_9H_7

Table 3: *Assigned ^{1}H- and ^{13}C-NMR Chemical Shifts (δ in ppm, Relative to Tetramethylsilane). ^{1}H spectra of OBO and of SBS Were Taken in $(CD_3)_2CO$ and $(CD_3)_2SO$ Solution, Respectively. All Other Spectra Were Taken in $CDCl_3$ Solution. See Figure 1 for Compound Numbering.*

	NBN	OBO	SBS		BNB	BOB	BSB
Heterocyclic Ring				**Phenyl Ring**			
C(2,X)	132.2	153.4	143.0	C(1,B)	137.9	137.1	137.0
C(3,X)	106.9	108.6	127.6	C(2,B)	126.0	126.4	126.4
H(3,X)	6.48	6.46	7.15	H(2,B)	7.44	7.48	7.46
C(4,X)	108.4	111.7	126.1	C(3,B)	128.7	128.7	128.7
H(4,X)	6.15	6.46	7.02	H(3,B)	7.32	7.34	7.34
C(5,X)	123.7	142.2	124.4	C(4,B)	127.1	127.6	127.7
H(5,X)	6.64	7.54	7.30	H(4,B)	7.20	7.23	7.25
Olefinic Link				**Olefinic Link**			
C(1,O)	116.7	116.4	121.8	C(1,O)	126.6	127.4	128.6
H(1,O)	6.96	7.04	7.32	H(1,O)	6.88	6.87	6.91
C(2,O)	125.8	126.8	128.0	C(2,O)	117.0	116.3	121.9
H(2,O)	6.85	6.97	6.91	H(2,O)	6.97	7.12	7.18
Phenyl Ring				**Heterocyclic Ring**			
C(1,B)	136.8	136.4	136.4	C(2,X)	133.8	153.0	142.0
C(2,B)	126.3	126.7	126.6	C(3,X)	107.8	111.2	128.0
H(2,B)	7.41	7.48	8.03	H(3,X)	6.54	6.38	6.95
Substituent				**Substituent**			
N-C̲H₃	34.1			N-C̲H₃	30.7		
N-CH̲₃	3.70			N-CH̲₃	3.70		

Nuclear Magnetic Resonance Spectroscopy

^{1}H- and ^{13}C-NMR spectra of the compounds in deuteriated chloroform solution were recorded at room temperature. A Varian Unity spectrometer operating at 400 MHz and 100 MHz respectively, was used in conjunction with a Sun Spark (Palo Alto, CA) data system. Tetramethylsilane was used as the internal standard. Chemical shift assignments are based on carbon-hydrogen 2D correlation spectra combined with standard knowledge of shifts, coupling constants and intensities[12], as well as previous work on similar compounds[13-15]. Table 3 shows the results. This set of data was then employed to determine the following substituent chemical shift increments (SCI values):

(i) SCI values describing the influence exercised by substituents of type $C_4H_3X\text{-}CH\text{=}CH\text{-}$ with X = S, O, NCH_3 on the chemical shifts of phenyl atoms (Table 4).

(ii) SCI values describing the influence exercised by a styryl ($C_6H_6\text{-}CH\text{=}CH\text{-}$) substituent on the chemical shifts of the heterocyclic ring atoms of type $C_4H_3X\text{-}$ with X = S, O, NCH_3 (Table 5).

(iii) SCI values describing the influence exercised by substituents of type $C_4H_3X\text{-}$ with X = S, O, NCH_3 on the chemical shifts of ethylenic atoms of type trans -CH=CH- (Table 6).

Table 4: *Shift Increments of $C_4H_3X\text{-}CH\text{=}CH\text{-}$ Substituents on the Chemical Shifts of a Phenyl Unit.*

	For ^{13}C-spectra				For ^{1}H-spectra		
	Z_{ipso}	Z_{ortho}	Z_{meta}	Z_{para}	Z_{ortho}	Z_{meta}	Z_{para}
X = S	+8.5	-2.1	+0.2	-0.8	+0.20	+0.08	-0.01
X = O [a]	+8.6	-2.1	+0.2	-0.9 [a]	+0.22	+0.08	-0.03
X = NCH_3	+9.4	-2.5	+0.2	-1.4	+0.18	+0.06	-0.06

[a] taken from ref. [11]

Such SCI can be of use to interpret NMR spectra of other molecules, but can also provide information about the electron donating/electron accepting properties of substituents via an inductive or mesomeric mechanism. The latter information is usually most reliably present in Z_{meta} for inductive, and in Z_{para} and Z_β values for mesomeric effects. Estimating the uncertainties in the tabulated SCI values at 0.05 for ^1H data and at 0.4 for ^{13}C data, we conclude from the results (Tables 4 - 6) the following. First, all $C_4H_3X\text{-}CH\text{=}CH\text{-}$ substituents are inductive electron acceptors, behaving in this aspect similarly as a $C_6H_6\text{-}CH\text{=}CH\text{-}$ group[9,12]. Unfortunately, the numerical values of Z_{meta} do not allow to put them in sequence. Second, the fact that all Z_β and Z_{cis} values are negative and all Z_α values are positive shows that $C_4H_3X\text{-}$ substituents are mesomeric donors[15]. Even though magnetic anisotropy and steric effects obscure the picture to a certain extent the data suggest that donor properties decrease in the order N-methylpyrrole > furan > thiophene. Third, it now could be expected, and is indeed observed, although not statistically significant, that Z_{para} and Z_{ortho} follow (Table 4) the same order, and hence mesomeric donor properties also decrease in the sequence $C_4H_3N(CH_3)\text{-}CH\text{=}CH\text{-}$ > $C_4H_3O\text{-}CH\text{=}CH\text{-}$ > $C_4H_3S\text{-}CH\text{=}CH\text{-}$. Fourth, it can be argued that the more a (heterocyclic) group mesomerically donates electrons, the least it will accept electrons by back-donation from a neigbouring styryl group. In accordance with this view one

Table 5: *Shift Increments of a Styryl Substituent on the Chemical Shifts of a $C_4H_3X\text{-}$ Heterocyclic Unit.*

	For ^{13}C-spectra				For ^{1}H-spectra		
	Z_{22}	Z_{23}	Z_{24}	Z_{25}	Z_{23}	Z_{24}	Z_{25}
X = S	+18.1	+1.2	-0.3	-0.5	+0.19	+0.06	+0.34
X = O	+10.4	-1.3	+1.8	-0.8 [a]	+0.16	+0.16	+0.16
X = NCH_3	+10.6	-1.1	+0.4	+2.1	+0.56	+0.23	+0.27

[a] taken from ref. [11]

notes (Table 5) that for Z_{25} the reverse order SCI (X = S) < SCI (X = O) < SCI (X = NCH_3) is generally followed.

Table 6: *Averaged Shift Increments of a C_4H_3X- Substituent on the Chemical Shifts of a $C^\alpha H=C^\beta H$- Unit (in Trans Configuration).*

	For ^{13}C-spectra		For ^{1}H-spectra	
	Z_α	Z_β	Z_{gem}	Z_{cis}
X = S	+16.0	-14.0	+1.30	+0.62
X = O	+14.8	-19.5	+1.29	+0.45
X = NCH$_3$	+13.9	-19.0	+1.27	+0.35

UV - Visible Spectroscopy

UV - visible spectroscopy of the compounds given in Figure 1 were recorded at room temperature on an Unicon UV-8451 spectrophotometer, using dilute solutions in methanol ranging in concentrations from $2x10^{-6}$ mol/l to $7x10^{-6}$ mol/l. Table 7 gives the absorption maxima and molar extinction coefficients. From the data the following emerges. First, λ_{max} value of an XBX compound varies with the nature of the peripheral heterocycle. Their sequence λ(NBN) > λ(OBO) > λ(SBS) shows the same order as found in the NMR data for the electron donor properties of N-methylpyrrole, furan and thiophene. In previous work Seus[11] stated that in the BXB series, the hetero-atom plays the role of a substituent and is no part of the chromophore. This means that the maximum absorption wavelength λ_{max} is independent of the type of central hetero-arylene. However, from our experimental spectra (see below, section electronic excitations), we find that λ_{max} (the 0-1 excitation) does depend on the type of heteroatom. Second, the regular heterocyclic trimers OOO and SSS have much higher λ_{max} values than the mixed heterocyclic trimers, and much higher than BBB. The sequence λ(regular heterocyclic trimers) > λ(BXB compounds) > λ(XBX compounds) > λ(BBB) suggests that the shape of the molecules is of importance.

Table 7: *UV-Visible Absorption Spectra of the Compounds in Methanol Solution; See Figure 1 for Abbreviations.*

Compound	λ_{max} (nm)	ε (l mol^{-1} cm^{-1})	Compound	λ_{max} (nm)	ε (l mol^{-1} cm^{-1})
NBN	376	$4.1x10^4$	BNB	385	$3.7x10^4$
OBO	365		BOB	380	$3.0x10^4$
SBS	372	$3.0x10^4$	BSB	385	$4.1x10^4$
OOO [a]	418	$1.5x10^4$	BBB [a]	359	
SSS [a]	410				

[a] taken from ref. [11]

CALCULATIONS

Here, we present the results of a semiempirical investigation of the geometry, electronic structure and electronic excitations of BXB and XBX compounds. As stated before, the AM1 method as implemented in MOPAC[16] was used to optimize the geometries of all molecules. These geometries were used in single point CNDO/S-CI[17] calculations as implemented in MOS-F[18]. The two-center electron repulsion integrals were approximated by the Ohno-Klopman (OK) formula. It is generally accepted that Hartree-Fock (HF) theory fails to produce accurate electronic excitations in molecules, and that it is necessary to go beyond this level. In Configuration Interaction (CI) methods a linear combination of Slater-determinants is used to describe the wavefunction of different states or configurations. In this way it is possible to correct for the correlation energy, which is neglected in the HF-theory. In order to calculate the electronic excitations a limited configuration interaction treatment is necessary. In the following CI calculations we include all singlet excitations between the 20 highest occupied orbitals and the 20 lowest virtual orbitals.

Geometry

We calculate for the series XBX and BXB the geometries and conformational energies of the possible symmetric conformers: the syn,syn- and the anti,anti-conformer. The nomenclature for these conformers is based on the relative position of the vinyl bonds with respect to the hetero-atom. In the syn,syn conformer, the vinyl bonds and the hetero-atom are on the same side of the molecule, while in the anti,anti conformer, the olefinic bonds and the hetero-atom are on different sides (see Fig. 2).
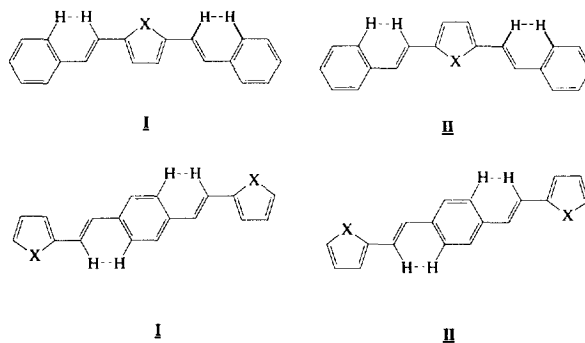
Figure 2: *Definition of anti,anti Conformation (I) and syn,syn Conformation (II) in BXB and XBX ompounds, Also Showing Steric Hindrance between Hydrogen Atoms.*

In the calculations no geometrical constraints were used and the geometry optimisation was deliberately started from a non-planar starting geometry, in order to avoid a possible local maximum at the planar structure. In fact, it can be expected that the optimized geometry is a compromise between the planar structure, favoured by π-conjugation effects, and the distorted structure, favoured by repulsion forces between the olefinic hydrogen atoms and the hydrogen atoms at the ortho-position of the phenyl rings, as depicted in Figure 2. In planar syn,syn and anti,anti conformers the distance between these two hydrogen atoms would be smaller than 2.4Å (two times the Van der Waals' radius of a hydrogen[19]). Indeed, the phenyl ring and the olefinic bond are not

coplanar in the optimized geometries (see Table 8). The dihedral angles range from 16.5° in the conformers of OBO to 23.2° in the syn,syn conformer of BNB. The dihedral angles between the heteroaryl ring and the olefinic bond are in general very small, except for the syn,syn conformers of BNB and NBN, where the steric hinderance of the methyl group causes the pyrrole ring to move out of the plane of the olefinic bond. In these cases, the dihedral angle is 28.7° and 26°, respectively.

The optimized geometries of the XBX oligomers show C_i symmetry in both the syn,syn and anti,anti conformers. In the BXB series, the syn,syn and anti,anti conformers all have C_s symmetry. Next, we calculated the rotational barriers to rotate the heterocyclic moiety from the anti,anti-form to the syn,syn-form. In Table 9 we summarize the relative conformational energies together with the rotational barriers. It follows that for each oligomer the anti,anti rotamer has the lowest energy, but the energy difference with the syn,syn form is very small. In fact, in comparison with ab-initio calculations and experimental data, AM1 calculated energy differences between conformers are often too small. Nevertheless, studies of Fabian [20] and of Belletête et al.[21] on conjugated molecules have shown that AM1 gives correct trends in conformational energies.

Table 8: *Torsion Angles (in degrees) Between the Phenyl Ring and the Vinyl Bond (Ph-C=C) and Between the Heteroaryl and the Vinyl Bond (X-C=C) for the Two Conformers.*

Compound	Torsion	syn,syn	anti,anti
BOB	Ph-C=C	17.6	17.4
	X-C=C	0.6	0.4
BSB	Ph-C=C	19.4	20.5
	X-C=C	2.2	3.2
BNB	Ph-C=C	23.2	22.2
	X-C=C	28.7	14.4
OBO	Ph-C=C	16.5	16.5
	X-C=C	0.0	0.0
SBS	Ph-C=C	17.7	19.5
	X-C=C	1.9	3.0
NBN	Ph-C=C	21.8	20.2
	X-C=C	26.0	4.6

Table 9: *Relative Energies of the Two Conformers and the Rotational Barrier (90°) of the Six Trimers (in kcal/mol).*

Molecule	anti,anti	90°	syn,syn
BOB	0.00	6.76	0.14
BSB	0.00	3.83	0.23
BNB	0.00	4.41	0.23
OBO	0.00	6.67	0.23
SBS	0.00	3.78	0.23
NBN	0.00	4.89	0.67

Electronic Structure

To interpret the properties of the molecular orbitals in the active space, which contribute to the electronic excitations, we use the LCAO-coefficients of the wavefunction. In the Roothaan approximation, molecular orbitals (ψ) are written as a linear combination of n atomic orbitals ϕ (LCAO-approximation, Roothaan). Furthermore, as a result of the neglect of differential overlap (NDO)-approximation (used in

$$\psi_k(r) = \sum_{i=1}^{A} C_{k,i}\phi_i(r) \tag{1}$$

AM1) and the fact that the wavefunction is normalised, the sum of squares of the LCAO-coefficients is equal to 1. Therefore, the square of the coefficient $C_{k,i}$ represents the contribution of the i-th atomic orbital to the k-th molecular orbital. We start to describe the topology of the molecular orbitals of the various oligomers, which are conformer independent. Table 10 gives an overview of the topologies of the ten molecular orbitals of the BXB and XBX trimers around the band gap. We see that all occupied orbitals have a π-character. The two highest occupied orbitals are delocalized over the whole molecule, whereas the other orbitals are localized on the rings. In the BXB molecules we note (i) two degenerate occupied orbitals which are localized on the phenyl ring, (ii) except for the LUMO+5 and LUMO+2 orbitals in BSB, all unoccupied (virtual) orbitals have a π^* character, (iii) the lowest virtual orbitals are delocalized over the whole molecule. All other virtual orbitals are localized on the phenyl groups.

Table 10: *Topologies of the Orbitals of BXB and XBX. All Orbitals have a π/π^* Character, Unless Otherwise Stated. d Means Delocalized, While l(X), X=S,O,N Means Localized on the Heterocycle. l(B) Means Localized on the Phenyl moiety.*

	BSB	BOB	BNB	SBS	OBO	NBN
LUMO+5	σ^*	d	d	σ^*	d	d
LUMO+4	d	d	d	d	d	σ^*
LUMO+3	d	l(B)	l(B)	d	d	d
LUMO+2	σ^*	l(B)	l(B)	l(B)	l(B)	l(B)
LUMO+1	d	d	d	d	d	d
LUMO	d	d	d	d	d	d
HOMO	d	d	d	d	d	d
HOMO-1	d	d	d	d	d	d
HOMO-2	l(S)	l(B)	l(N)	l(S)	d	l(N)
HOMO-3	l(B)	l(B)	l(B)	l(S)	l(B)	l(N)
HOMO-4	l(B)	d	l(B)	l(B)	l(O)	d
HOMO-5	d	l(O)	d	d	l(O)	l(B)

In the XBX molecules we note: (i) two degenerate orbitals localized on the heterocyclic ring within the 5 highest occupied orbitals, along with one occupied orbital, localized on the phenyl ring. (ii) among the virtual orbitals, there are two low lying σ^* orbitals (LUMO+5 of SBS and the LUMO+4 of NBN). The other virtual orbitals all have π* character, (iii) all virtual orbitals are delocalized over the whole molecule except the LUMO+2 orbitals which are localized on the phenyl rings. It is important to note that in the BXB series the heteroatom does not contribute to the HOMO orbital. This is due to the symmetry of the molecule. In the HOMO orbital, the heteroatom is lying in a nodal plane. This has some repercussion on the first electronic excitation.

Next, we turn the attention to the charge distribution in the molecules. In Figure 3, we compare the electron densities in a parent heteroaromatic compound with those in the appropriate heterocyclic parts of BXB and XBX. It shows that charge distributions of N-methylpyrrole and furan are comparable. The highest electron density is situated at the 3 and 4 positions, while the carbons at positions 2 and 5 and the heteroatom are less negative. The nitrogen atom in N-methylpyrrole is more negative than the oxygen in furan. In thiophene the carbons at position 2 and 5 have the highest electron-density while the sulphur atom is
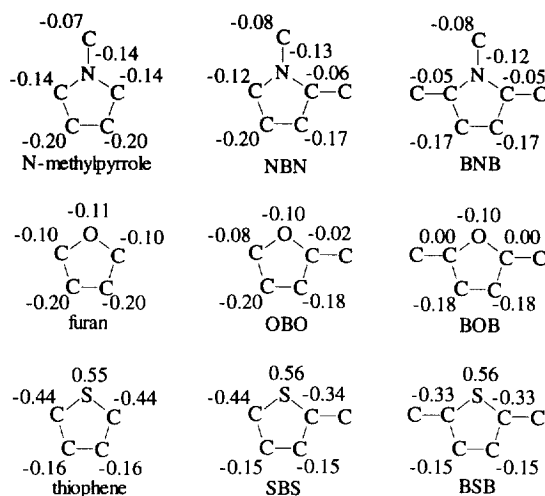
Figure 3: *AM1 Calculated Charge Densities in the Parent Heterocycles and in the Heterocyclic Moieties of XBX and BXB Compounds.*

positively charged. Monosubstitution (in the case of XBX) and disubstitution (in BXB) leave the charges of most atoms quasi unchanged. Substitution only significantly changes the electron density on the carbon atoms that are directly attached to the substituent. We may conclude that the electron density increases in the order sulphur (thiophene) < oxygen (furan) < nitrogen (N-methylpyrrole), and conclude that the electron donating properties increase in the same order. In this way, we can explain our findings in the NMR spectra.

Electronic excitations

Tables 11 and 12 give an overview of the excitation energies E_{exc}, oscillator strengths f, dipole moments of the excited states μ, excitation symmetry S and assignments for the calculated singlet excitations of the two conformers of the NBN and the BNB compounds. The first 10 singlet-singlet excitations are included. The molecules are positioned in such a way that the long molecular axis is along the x-axis of the system and the short axis along the y-axis. In this way, we can examine the three parts of the excited dipole moment within the framework of the molecular geometry. The excitations presented in these tables are characteristic for XBX and BXB series, respectively, and show a clear distinction between the XBX and BXB series.

Because of the C_i symmetry of the XBX series, the spectra of both the anti,anti and the syn,syn conformer only have A_u excitations, A_g excitations being symmetry forbidden (see Table 11). The A_u excitations occur between states with different symmetry ($A_g \rightarrow A_u$ or $A_u \rightarrow A_g$). When one compares the spectra of both conformers, one notes that the oscillator strengths do not change significantly for the same excitations in the two conformers. Both conformers of XBX molecules have quasi zero dipole moments in the ground state and excited state.

Table 11: Assignment of the 10 Lowest Singlet-Singlet Excitation Energies in NBN. A Comparison Between the Syn,Syn- and Anti,Anti-Conformer. Excitation Energy E_{exc} in eV, Oscillator Strength f in Arbitrary Units, Excitation Symmetry S and Dipole Moments of the Excited State μ in Debye.

syn,syn

E_{exc}	f	μ	μ	μ	S	Assignment
3.272	1.496	-0.001	-0.002	-0.002	A_u	69% HOMO→LUMO; 20% HOMO-1→LUMO+1
3.932	0.000	0.000	-0.003	-0.002	A_g	42% HOMO→LUMO+1; 35% HOMO-1→LUMO; 11% HOMO-1→LUMO+3
4.409	0.012	-0.001	-0.002	0.002	A_u	44% HOMO→LUMO+2; 24% HOMO-5→LUMO; 19% HOMO-1→LUMO+2
4.601	0.053	-0.000	-0.002	-0.002	A_u	32% HOMO→LUMO+3; 15% HOMO-2→LUMO; 15% HOMO-1→LUMO+1; 15% HOMO-5→LUMO+2
4.954	0.000	0.000	-0.004	-0.001	A_g	22% HOMO→LUMO+4; 17% HOMO-1→LUMO+5; 13% HOMO-4→LUMO+1
5.000	0.005	-0.001	-0.002	-0.004	A_u	18% HOMO→LUMO+5; 16% HOMO-3→LUMO+1; 15% HOMO-1→LUMO+4
5.451	0.000	0.003	-0.003	-0.002	A_g	37% HOMO-1→LUMO; 14% HOMO-1→LUMO+3; 9% HOMO→LUMO+6
5.624	0.523	-0.002	-0.002	-0.002	A_u	25% HOMO-5→LUMO+2; 13% HOMO→LUMO+7; 9% HOMO-1→LUMO+6
5.658	0.000	0.000	-0.003	-0.003	A_g	24% HOMO-2→LUMO+1; 23% HOMO→LUMO+1; 14% HOMO→LUMO+4
5.903	0.154	-0.001	-0.002	-0.002	A_u	35% HOMO-2→LUMO; 12% HOMO→LUMO+3; 11% HOMO-6→LUMO+1

anti,anti

E_{exc}	f	μ	μ	μ	S	Assignment
3.128	1.496	-0.001	-0.001	-0.003	A_u	70% HOMO→LUMO; 20% HOMO-1→LUMO+1
3.811	0.000	0.000	-0.001	-0.003	A_g	43% HOMO→LUMO+1; 37% HOMO-1→LUMO; 9% HOMO-1→LUMO+3
4.392	0.013	0.001	-0.001	0.003	A_u	46% HOMO→LUMO+2; 24% HOMO-5→LUMO; 17% HOMO-1→LUMO+2
4.604	0.033	0.000	-0.001	0.003	A_u	33% HOMO→LUMO+3; 15% HOMO-1→LUMO+1; 15% HOMO-5→LUMO+2; 14% HOMO-2→LUMO
4.962	0.000	-0.001	-0.003	0.003	A_g	21% HOMO→LUMO+4; 17% HOMO-1→LUMO+5; 13% HOMO-4→LUMO+1
5.002	0.002	0.001	-0.001	0.005	A_u	19% HOMO→LUMO+5; 16% HOMO-3→LUMO+1; 15% HOMO-1→LUMO+4
5.370	0.000	0.000	-0.001	0.003	A_g	36% HOMO-1→LUMO; 15% HOMO-1→LUMO+3; 11% HOMO→LUMO+1
5.580	0.000	0.000	0.000	0.003	A_g	22% HOMO-2→LUMO+1; 19% HOMO→LUMO+1; 18% HOMO→LUMO+4
5.583	0.369	0.001	-0.003	0.002	A_u	24% HOMO-5→LUMO+2; 11% HOMO→LUMO+7; 11% HOMO-1→LUMO+4
5.938	0.137	0.001	-0.002	0.003	A_u	36% HOMO-2→LUMO; 16% HOMO→LUMO+5; 8% HOMO→LUMO+5

Table 12: *Assignment of the 10 Lowest Singlet-Singlet Excitation Energies in BNB. A Comparison Between the Syn,Syn- and Anti,Anti-Conformer. Excitation Energy E_{exc} in eV, Oscillator Strength f in Arbitrary Units, Excitation Symmetry S and Dipole Moments of the Excited State μ in Debye.*

Syn,syn							anti,anti						
E_{exc}	f	μ			S	Assignment	E_{exc}	f	μ			S	Assignment
3.118	0.979	0.001	0.097	0.293	A"	80% HOMO→LUMO 8% HOMO-1→LUMO+1	3.018	1.325	0.000	0.795	-0.037	A"	81% HOMO→LUMO
4.192	0.379	0.001	0.815	0.337	A'	57% HOMO→LUMO+1 12% HOMO-1→LUMO	4.121	0.027	-0.002	1.815	-0.070	A'	59% HOMO→LUMO+1 13% HOMO-1→LUMO
4.627	0.001	0.563	0.577	0.308	A'	20% HOMO-1→LUMO+3 19% HOMO→LUMO+2 14% HOMO-2→LUMO+2	4.620	0.000	-0.146	1.383	-0.056	A'	15% HOMO-1→LUMO+1 15% HOMO-3→LUMO+1 12% HOMO→LUMO+3
4.627	0.009	-0.565	0.569	0.867	A'	20% HOMO-1→LUMO+2 19% HOMO→LUMO+3 15% HOMO-2→LUMO+3 15% HOMO-5→LUMO+2	4.620	0.007	0.147	1.418	-0.032	A'	15% HOMO-1→LUMO+3 15% HOMO-4→LUMO+1 12% HOMO→LUMO+2 11% HOMO-3→LUMO
4.712	0.004	0.000	0.897	0.277	A"	26% HOMO→LUMO+4 16% HOMO-1→LUMO+1 13% HOMO-2→LUMO	4.733	0.011	0.002	1.413	-0.037	A"	26% HOMO→LUMO+4 16% HOMO-1→LUMO+1 12% HOMO-5→LUMO
4.793	0.000	0.000	1.591	0.291	A'	20% HOMO→LUMO+5 17% HOMO-1→LUMO 13% HOMO-2→LUMO+1	4.801	0.000	-0.003	2.300	-0.037	A'	20% HOMO→LUMO+5 16% HOMO-3→LUMO+1
5.399	0.207	0.050	-1.224	0.548	A'	30% HOMO-5→LUMO 20% HOMO→LUMO+1 19% HOMO→LUMO+7	5.292	0.075	-0.004	0.658	0.113	A'	36% HOMO-5→LUMO 12% HOMO→LUMO+7 10% HOMO→LUMO+1
5.479	0.191	-0.041	-0.895	0.416	A"	38% HOMO→LUMO+6 13% HOMO→LUMO+4	5.548	0.281	-0.141	-0.111	-0.025	A"	34% HOMO→LUMO+6 24% HOMO→LUMO+4
5.618	0.359	-0.010	2.336	0.018	A'	40% HOMO-1→LUMO 12% HOMO-1→LUMO+4 8% HOMO→LUMO+5	5.555	0.019	0.144	1.875	-0.014	A'	40% HOMO-1→LUMO 11% HOMO→LUMO+1 11% HOMO→LUMO+5 11% HOMO-1→LUMO+4
5.967	0.276	0.001	1.440	0.354	A'	31% HOMO-2→LUMO 8% HOMO→LUMO+4 8% HOMO-1→LUMO+5	6.022	0.275	0.002	2.266	-0.102	A'	28% HOMO-2→LUMO 9% HOMO-1→LUMO+5 8% HOMO→LUMO+4

In the BXB series, the spectra of both conformers show significant differences (see Table 12). In the spectra of the syn,syn conformers, the oscillator strengths of some higher energy excitations increase (e.g. the HOMO-5→LUMO excitation at $E_{exc.}$=5.29eV: f=0.075 in anti,anti increases to f=0.207 in syn,syn. The HOMO-1→LUMO excitation at $E_{exc.}$=5.56eV: f=0.019 in anti,anti increases to f=0.359 in syn,syn). At the same time the oscillator strength of the HOMO→LUMO exitation decreases in the syn,syn conformer. This causes the theoretical syn,syn spectrum to show more features.
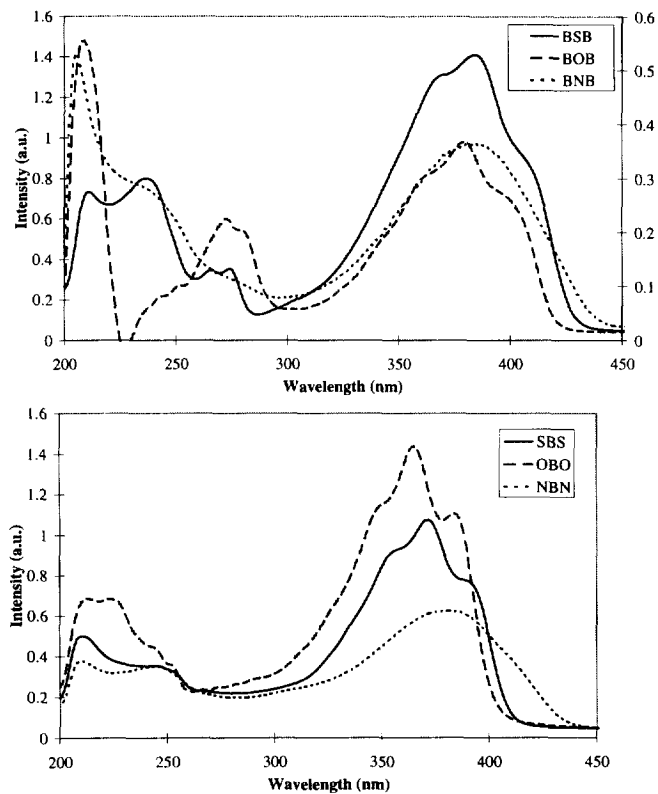
Figure 4: *The Experimental Spectra of the BXB (top) and XBX (bottom) Series.*

We want to draw attention to the fact that in the BXB series two types of excitations can be distinguished. The excitations with the lowest symmetry (A") have transition dipole moments along the long axis of the molecule. In this type of excitations, the source and destination state have different symmetries. The excitations with the highest symmetry (A') have transition dipole moments along the short axis of the molecule. In this type of excitations, both source and destination state belong to the same representation (have the same symmetry). There is no direct relation between the symmetry of the excitation and the increase in transition dipole moment.

In Table 13 we compare the calculated first singlet-singlet excitation energies of the two conformers with the experimental 0-0 and 0-1 excitations. We consider the λ_{max} to be the 0-1 wavelength, and the shoulder at higher wavelength (lower excitation energy) to be the 0-0 excitation. Due to peak broadening in the NBN and

BNB spectra, the determination of the position of the 0-0 shoulder is not straightforward. Although a detailed analysis of the spectra of the two series will be given later[22] we give here some preliminary results. In order to compare theoretical and experimental excitation energies, we have to consider the following. Relaxation of the atomic framework and the electronic wavefunction are neglected in the calculation of the electronic excitations: the excitations are vertical Koopmans' excitations. However, when these relaxations are small in the real systems, we can compare the theoretical excitation energies with the experimental 0-0 energies.

Table 13 shows that the calculated wavelengths agree best with the experimental 0-0 wavelengths. Furthermore, the calculated syn,syn wavelengths fit slightly better than the calculated anti,anti wavelengths. Also the band structure in the spectra of the syn,syn conformers is in better agreement with the experimental results. However, in view of the small differences in agreement between observed and calculated spectra as well as the small calculated energy differences between the syn,syn- and anti,anti-conformers, we believe that the observed spectra are due to mixtures of both conformers.

In contrast to the other compounds, we also see that the two conformers of NBN and BNB show a large difference in HOMO→LUMO excitation energy (15 nm) which is ascribed to the large deviation from planarity between the heterocycle and the vinyl bond. It is probably not due to a non-planar arrangement of the olefinic bond and the phenyl ring, because the dihedral angles between these moieties are almost equal for both conformers. For the other compounds the differences are much smaller. Figure 4 gives the experimental UV/Vis spectra of the six oligomers. From this Figure and Table 13 we see that the experimental λ_{max} values for the BXB series are not independent of the central heterocycle. From a theoretical viewpoint, we can state that although the heteroatom does not contribute to the HOMO orbital, the first excited state is a linear combination of the HOMO→LUMO and HOMO-1→LUMO+1 configurations. There is no indication that the latter configurations are independent of the heterocycle. Therefore, the excitation energies are not the same.

Table 13: *Comparison of the Calculated First Singlet-Singlet Excitation Absorption Wavelengths of the Two Conformers and the Experimental 0-0 and 0-1 Wavelengths (in nm)* .

	syn,syn	anti,anti	Exp. 0-1	Exp. 0-0
SBS	393	398	372	393
OBO	387	392	365	386
NBN	379	395	376	400
BSB	422	426	385-380[a]	409
BOB	412	410	380-379[a]	402
BNB	397	411	385-379[a]	400

[a] Reported by Seus [11]

CONCLUSION

By means of the Wittig reaction we prepared two series of hetero-arylene trimers 1,4-bis-[2-(heteroaryl-2-yl)ethenyl]benzenes (XBX) and 2,5-distyrylheteroarylenes (BXB) with N-methylpyrrole, furan and thiophene as hetero-aromatic groups. These compounds were characterized by mass spectroscopy, NMR and UV/Vis spectroscopy. Semiempirical calculations using AM1 and CNDO/S-CI proved to be useful to rationalize the findings of the NMR and UV/Vis spectra. Hereby, we focussed on the differences in the electronic spectra of the two series of trimers. The differences can be assigned to differences in the geometry (and symmetry) of these compounds. Moreover, the excitations are dependent of the conformation in the XBX series. Both from our

experimental UV/Vis spectra and the semiempirical calculations, we have conclude in contrast to Seus' hypothesis that in the BXB series as well as in the XBX series the λ_{max} is dependent of the type of central heterocycle.

ACKNOWLEDGEMENT

REFERENCES

1.   Dewar, M.J.S.; Zoebisch, E.G.; Healy, E.F.; Stewart, J.J.P. *J. Am. Chem. Soc.* **1985**, 107, 3902-3909.

2.   Saikachi, H.; Ogawa, H.; Minami, Y.; Sato, K. *Chem. and Pharm. Bull. (Japan)* **1970**, 18, 465-473.

3.   Cresp, T.M.; Sargent, M.V. *J. Chem. Soc. Perkin Trans. 1* **1973**, 23, 2961-2971.

4.   Elix, J.A.; Sargent, M.V. *J. Am. Chem. Soc.* **1968**, 90, 1631-1634.

5.   Elix, J.A. *Austr. J. Chem.* **1969**, 22, 1951-1962.

6.   Feringa, B.L.; Hulst, R.; Rikers, R. *Synthesis* **1988**, 316-318.

7.   Oleinik, A.F.; Novitskii, Yu K. *Otkrytiya Isobret. Obraztsy, Tovarnye Znaki* **1970**, 30, *USSR Patent* nr. 282331

8.   Novitskii, Yu K.; Volkov, V.P.; Yur'ev, Yu K. *J. General Chem. USSR*, I **1961**, 31, 538-. English transl. p. 494-.

9.   De Schrijver, D. *Synthese en Karakterisatie van Furanhoudende Oligomeren en Polymeren (in Dutch)*; University of Antwerpen (UIA): Belgium, 1989.

10. Sprangler, C.W.; Holl, T.J.; Sopochak, L.S.; Liu, P.K. *Polymer* **1989**, 30, 1166-.

11. Seus, E.J. *J. Heterocyclic Chem.* **1965**, 2, 318-320.

12. Pretsch, E.; Clerc, T.; Seibl, J.; Simon, W. *Tabellen zur Strukturaufklärung organischer Verbindungen mit spektroskopischen Methoden*; Springer: Berlin, 3rd Ed., 1990

13. Yang, Z. ; Geise, H.J. *Synth. Met.* **1992**, 47, 95-104.

14. Nouwen, J.; Vanderzande, D.; Martens, H.; Gelan, J.; Yang, Z.; Geise, H.J. *Synth. Met.* **1992**, 46, 23-44.

15. Jacobs, S.; Eevers, W.; Verreyt, G.; Geise, H.J.; De Groot, A.; Dommisse, R. *Synth. Met.* **1993**, 61, 189-193.

16. Stewart, J.J.P. *MOPAC, Program 455, Quantum Chemistry Program Exchange*, University of Indiana, Bloomington, IN.

17. Del Bene, J.; Jaffé, H.H. *J. Chem. Phys.* **1968**, 48, 1807-1813; Del Bene, J.; Jaffé, H.H. *J. Chem. Phys.*, **1968**, 48, 4050-4055

18. Matsuura, A.; Hayano, T. *Fujitsu Sci. Tech. J.* **1992**, 28, 402-412; Matsuura, A, *MOS-F, Program 651, Quantum Chemistry Program Exchange*, University of Indiana, Bloomington, IN.

19. *Handbook of Chemistry and Physics*, 52nd Ed. ,CRC, 1971.

20. Fabian, W.M.F. *J. Comp. Chem.* **1988**, 9, 369-377.

21. Belletête, M.; Leclerc, M.; Durocher, G. *J. Chem. Phys.* **1994**, 98, 9450-9456.

22. Thys, G.J.H; Van der Looy, J.F.A.; Van Alsenoy, C.; Geise, H.J. *to be published*